



HHS Public Access

Author manuscript

Nat Commun. Author manuscript; available in PMC 2015 September 27.

Published in final edited form as:

Nat Commun. ; 6: 6696. doi:10.1038/ncomms7696.

Global migration of influenza A viruses in swine

Martha I. Nelson^{1,*}, Cécile Viboud¹, Amy L. Vincent², Marie R. Culhane³, Susan E. Detmer⁴, David E. Wentworth^{5,#}, Andrew Rambaut^{1,6,7}, Marc A. Suchard⁸, Edward C. Holmes⁹, and Philippe Lemey¹⁰

¹Division of International Epidemiology and Population Studies, Fogarty International Center, National Institutes of Health, Bethesda, MD 20892 USA

²Virus and Prion Diseases of Livestock Research Unit, National Animal Disease Center, USDA-ARS, Ames, IA 50010 USA

³University of Minnesota Veterinary Diagnostic Laboratory, St. Paul, MN 55108 USA

⁴Western College of Veterinary Medicine, University of Saskatchewan, Saskatchewan, Canada

⁵J Craig Venter Institute, Rockville, MD USA 20850 USA

⁶Institute of Evolutionary Biology, University of Edinburgh, Ashworth Laboratories, Edinburgh, EH9 5LT United Kingdom

⁷Centre for Immunology, Infection and Evolution, University of Edinburgh, Ashworth Laboratories, Edinburgh, EH9 5LT United Kingdom

⁸Departments of Biomathematics and Human Genetics, David Geffen School of Medicine at UCLA, and Department of Biostatistics, UCLA School of Public Health, Los Angeles, CA 90095 USA

⁹Marie Bashir Institute for Infectious Diseases and Biosecurity, Charles Perkins Centre, School of Biological Sciences and Sydney Medical School, University of Sydney, NSW 2006, Australia

¹⁰Department of Microbiology and Immunology, Rega Institute, KU Leuven – University of Leuven, Leuven, Belgium

Users may view, print, copy, and download text and data-mine the content in such documents, for the purposes of academic research, subject always to the full Conditions of use:http://www.nature.com/authors/editorial_policies/license.html#terms

*Corresponding author: Division of International Epidemiology and Population Studies, Fogarty International Center, National Institutes of Health, 16 Center Drive, Building 16, Room 202, Bethesda, MD 20892 USA. Tel: 1 301-402-5203; Fax: 1 301-496-8496; nelsonma@mail.nih.gov.

#Current address: Influenza Division, National Center for Immunization and Respiratory Diseases, Centers for Disease Control and Prevention, Atlanta, Georgia, United States of America

Author contributions

Generated the data used in the analysis: MRC SED DEW. Conceived, designed, and performed the analysis: MIN CV PL. Analyzed the data: MIN CV ECH PL. Wrote the paper: MIN CV ALV MRC SED DEW AR MAS ECH PL. The opinions expressed in this article are the author's own and do not reflect the view of the Centers for Disease Control and Prevention, the Department of Health and Human Services, or the United States government.

Competing interests

The authors have declared that no competing interests exist.

Accession codes

All sequences from swine influenza A viruses that were generated and used in this study have been deposited in the GenBank database with the accession codes AHB20822 to AHB20891, AHB20919 to AHB23256, AHB23664 to AHB23860, AHB24418 to AHB24833, and AHB82076 to AHB82086.

Abstract

The complex and unresolved evolutionary origins of the 2009 H1N1 influenza pandemic exposed major gaps in our knowledge of the global spatial ecology and evolution of influenza A viruses in swine (swIAVs). Here we undertake an expansive phylogenetic analysis of swIAV sequence data and demonstrate that the global live swine trade strongly predicts the spatial dissemination of swIAVs, with Europe and North America acting as sources of viruses in Asian countries. In contrast, China has the world's largest swine population but is not a major exporter of live swine, and is not an important source of swIAVs in neighboring Asian countries or globally. A meta-population simulation model incorporating trade data predicts that the global ecology of swIAVs is more complex than previously thought, and the US and China's large swine populations are unlikely to be representative of swIAV diversity in their respective geographic regions, requiring independent surveillance efforts throughout Latin America and Asia.

Introduction

In early 2009, a novel reassortant H1N1 influenza A virus with gene segments from two swine virus (swIAV) lineages emerged in humans, initiating the first influenza pandemic of the 21st century. The virus had a complex genetic composition that had not been previously detected in swine, with six genome segments of North American triple reassortant swine virus origin (PB2, PB1, PA, HA (H1), NP, and NS) and two genome segments of Eurasian avian-like swine virus origin (NA (N1) and MP)¹. Evolutionary analysis of this novel North American/Eurasian reassortant virus indicated that these segments had circulated undetected in swine for at least eight years². The first human outbreak of the pandemic H1N1 virus (pH1N1) occurred in Mexico, and the extent of viral genetic diversity observed in Mexico supports the hypothesis that the virus first emerged there in humans³. However, efforts to detect the last common ancestor of the pH1N1 virus in Mexican swine populations have not been successful to date, and the opaque evolutionary history of the pandemic virus in swine highlights the gaps in our understanding of swIAV dynamics at a global scale.

In general, influenza viruses in swine are spatially separated into distinct North American and European swIAV lineages, although viruses of North American and European origin both circulate in Asia. Multiple viral lineages co-circulate in North American swine, including (i) 'classical' swine viruses, which descend from the 1918 H1N1 pandemic⁴; (ii) 'triple reassortant' swine viruses, which emerged in the mid-1990s with a combination of human, swine, and avian segments⁵; and (iii) 'delta' (δ) viruses that are closely related to human seasonal H1 viruses from the early 2000s^{6,7}. The main European swIAV lineages include 'avian-like' H1N1 viruses that jumped from birds to swine in the 1970s, human-origin H1N1 viruses from the 1980s, and human-origin H3N2 viruses that are antigenically described as A/Port Chalmers/1/1973-like⁸. Multiple North American and European-origin swIAV lineages have both been identified in Asian countries^{9–12}. Due to high levels of co-infection, segmental reassortment occurs frequently in swine, such that they are an important reservoir host for influenza virus genetic diversity^{9,11,13–16}.

Live transport is routine in swine farming, and in the United States the transport of millions of swine from Southern to Midwestern regions for end-stage production appears to drive the

strongly directional dissemination of swIAVs from Southern US states with high hog production (e.g., North Carolina, Texas, and Oklahoma) to the traditional center of swine farming located in the Midwestern ‘corn belt’¹⁷. Large numbers of swine also enter the United States from Canada, which has been implicated in the dissemination of other important swine pathogens, including Porcine Reproductive and Respiratory Syndrome Virus (PRRSV)¹⁸. Intercontinental trade of live swine also occurs, for end-stage production or to acquire female breeding pigs for genetic improvement of swine reproduction or growth traits. Globally, the largest swine population is found in China, where over 450 million hogs reside (Fig. 1). Large swine populations also are found in the United States (> 60 million hogs), Brazil (> 30 million hogs), Vietnam (> 20 million hogs), Germany (> 20 million hogs), and Spain (> 20 million hogs).

Despite the global nature of both swine farming and swIAV circulation, the patterns and dynamics of the worldwide spread of this economically important virus are unknown. To characterize the phylodynamics and phylogeography of swIAVs at a global scale, here we conduct a phylogenetic analysis of 785 whole-genome swIAV sequences collected from ten countries/regions representing four continents, the largest study of its kind undertaken to date. To assess the drivers of viral migration, we compare the phylogeographic patterns with empirical data on live swine trade and swine population sizes. Based on these findings, we build a meta-population model to simulate the spatial dissemination of swIAVs at a global scale and identify regions at high risk for co-invasion of divergent lineages, increased total genetic diversity, and emergence of viruses with pandemic potential.

Results

Global migration of swIAVs

Phylogenetic analysis revealed that long-distance movement of influenza A viruses between countries and continents has occurred continuously in swine since the 1970s (summarized in Fig. 2). Our estimate of 18 international viral migration events is a minimum based on the currently available influenza virus sequence data and certainly underestimates the true number. This lower-bound estimate is based on discrete monophyletic groups (defined by country) that are supported by high posterior probabilities (> 80), reflecting migration events that led to successful onward transmission. The estimate does not include the much higher number of international viral movements between the United States and Canada or between countries in Europe, which are each considered as meta-populations in our analysis. The estimate also does not consider viral migration events for which only one sequence is available, any viruses that do not form a well-supported clade, or which only partial sequence data was available.

Although global surveillance and sequencing of swIAVs has increased dramatically in the last five years, our time-scaled MCC phylogenies indicate that most intercontinental viral migration events occurred prior to this increase in surveillance (representative phylogeny of the NA segment is presented in Fig. 3; phylogenies for other seven segments are available in Supplementary Figs. 1–7). Eight of the 18 viral migration events identified in our study were evident on the phylogenies inferred for all eight viral genome segments, indicative of onward transmission of the full viral genome in the new location (introductions 1, 3, 4, 5, 8,

9, 10, 15). The consistency of spatial-temporal inferences across these eight segments strengthens inferences of when and where each of these introductions occurred (Supplementary Table 1). Ten viral migration events could only be identified by a subset of genome segments, as at least one segment has been replaced in intervening years by reassortment (introductions 2, 6, 7, 11, 12, 13, 14, 16, 17, and 18). There is no evidence in these data that either of the 8-1 or 8-2 virus lineages that emerged in North American swine in the early 2000s has transmitted to swine on any other continents, despite high rates of detection in US swine populations of 8-1 viruses¹⁹.

A consistent global spatial dynamic was observed for swIAVs during 1970–2013, based on both a conservative measure of strongly supported monophyletic groups (Fig. 3 and Supplementary Figs. 1–7) as well as ‘Markov jump’ counts²⁰ of the expected number of location state transitions along the branches of the tree. ‘Markov jump’ counts provide a quantitative measure of gene flow between regions that includes singletons and clusters that may have poor phylogenetic resolution (Fig. 4, Supplementary Table 2). Overall, North America (in this case referring to the United States and Canada) and Europe represent independent viral source populations for the Asian countries sampled in our study: China, Japan, South Korea, Thailand, and Vietnam. In contrast, only a single swIAV migration event was observed between North America and Europe (introduction 5).

Spatial dynamics of swIAVs in North America—Bi-directional viral migration between Canada and the United States is so frequent (reflected by the extremely high number of Markov jump counts, Fig. 4) that Canada and the US were considered as a single meta-population, similar to Europe (Fig. 2). The higher availability of swIAV sequence data from US swine makes it particularly difficult to distinguish whether an introduction was specifically of US or Canadian swine origin, and the origin of such introductions is more appropriately characterized as ‘North American’. Using newly generated sequence data from five swIAVs of the H3N2 subtype that were collected in Mexico during 2010–2011 (A/sw/Mexico/SG1442/2010, A/sw/Mexico/SG1444/2011, A/sw/Mexico/SG1447/2011, A/sw/Mexico/SG1448/2011, and A/sw/Mexico/SG1449/2011, accession numbers available in Supplementary Table 3), our phylogenetic analysis provides evidence of a single introduction of a H3N2 triple reassortant swIAV from the United States into Mexico that occurred between mid-2005 and mid-2006 (introduction 11, Fig. 2). At the time of sampling, all five Mexican swIAVs had acquired at least one pH1N1 segment of human origin via reassortment, evidence that pH1N1 viruses also have circulated in Mexico’s swine population.

Spatial dynamics of swIAVs in Asia

Given China’s large swine population and long-term surveillance, it may have been expected that this country (encompassing mainland China, Hong Kong, Taiwan, and Macau) would be an important source of swIAV diversity for neighboring Asian countries in this study. However, since 1970 there have been 16 swIAV introductions of European or North American origin into Asia, compared to only two swIAV migration events between Asian countries, and only one definitive introduction of a swIAV from China into another country (introduction 16). Overall, the genetic diversity of swIAVs in Asia derives from five swIAV

introductions of European origin and eleven swIAV introductions of North American origin. Six viral introductions from Europe and North America were observed in Thailand, and five introductions were observed in China, including the earliest intercontinental swIAV migration detected to date (introduction 1, Fig. 2).

In contrast to the frequent exchange of swIAVs across European country borders and across the US-Canadian border, only two swIAV migration events were observed between any two Asian countries. A pair of H1 segments collected in South Korea in 2013 are positioned within a clade of avian-origin Eurasian viruses from China, suggesting China-to-Korea migration (introduction 16, Fig. 2 and Supplementary Fig. 4). Closely related North American triple reassortant viruses also were identified in China and Vietnam, suggestive of viral migration between these Asian countries. However, the location state probability for the node representing the common ancestor of the Chinese and Vietnamese clades is too low (ranging from 0.46 to 0.65 across the eight genome segments) to determine whether the North American virus was first introduced to Vietnam and disseminated to China, or vice versa (Fig. 2 and Supplementary Figs. 1–7).

Although much of the swIAV diversity in Asia appears to have emerged in the last two decades, the phylogenies suggest long-term circulation of swIAVs in Thailand and Japan, either via imports from North American or European swine in the 1970s and 1980s (Fig. 2) or direct introductions from humans as early as the 1960s (Fig. 3c). Long branch lengths and the lack of historical swIAV data from Asian countries make it difficult to infer with confidence the spatial history of older viral lineages in Asia. The relative lack of swIAV surveillance in Thailand prior to 2000 particularly complicates estimates of the timing and spatial pathway of the multiple viral introductions from North America and Europe that likely occurred during the 1980s and 1990s (e.g., introductions 6, 14, 17, and 18). At this time, there is little evidence of viral dissemination from Japan or Thailand to other Asian countries in our study, despite many decades of potential swIAV circulation. However, the relatively long branches may not reflect a single direct transition between the origin and (final) destination location, and may conceal additional spatial movements during the elapsed time. The evolutionary history of swIAVs in Thailand is also made more complex by the frequency of reassortment involving multiple clades, poorly supported clusters, and singletons. Whereas avian-like Eurasian viruses in China are monophyletic and result from a single introduction from Europe (introduction 15), the Thai viruses from this lineage are monophyletic only in the PB2, NP, and N1 trees. Our estimate of two introductions of avian-like Eurasian viruses into Thailand is therefore conservative and likely underestimates the true number (introductions 13 and 14, Figs. 2 and 3, Supplementary Figs. 1–7). Singletons and unsupported clusters also were observed among South Korean viruses, complicating the estimation of the number of viral migration events into South Korea as well.

Importance of live swine trade in the global dispersal of swIAVs

We used a generalized linear model (GLM) extension of phylogeographic inference²¹ to identify the putative drivers of swIAV migration events inferred from the genetic data. This approach considers single introductions and clusters that may have poor resolution, the uncertainty of which is accommodated by the analysis. The Bayesian model averaging

approach found consistent and strong evidence that the amount of asymmetric live swine trade (measured in USD for the years 1996–2012) from one country to another is the dominant driver of the dispersal of IAVs in swine globally. This is reflected by the maximal estimated inclusion probability of live swine trade for all six internal gene segments (probability of 1, results for PB2, PB1, PA, and NP are presented in Fig. 5; results for the shorter MP and NS segments are available in Supplementary Fig. 8; the analysis could not be performed on the HA or NA due to the high frequency of human viruses in these phylogenies). Accordingly, viral migration, measured by ‘Markov jump’ counts, was positively correlated with live swine trade volume (USD) ($\rho = 0.52$, $p = 1.5 \times 10^{-7}$, Spearman correlation, Supplementary Fig. 9).

Other potential predictors, including swine population size, contributed little to the observed global spatial patterns, except for the number of sequences of the country of destination (average probability of ~0.5 across the six internal segments). Not only is the effect of live swine trade consistently robust to the inclusion of sample size, the high inclusion probability of live swine trade in cases where the effect of sample size is particularly low (e.g., the PA segment) indicates that it is also independent of sample size. The conditional effect size (the size of the effect conditional on the predictor being included in the model) ranges between about 3 to 5 on a log scale, implying that viral lineage movement probability is several orders of magnitude higher for connections with the highest swine trade compared to connections without trade (Fig. 5).

Our GLM analysis could be affected by regional differences in the early establishment of swIAVs, with swIAVs having been potentially seeded later in Asia and decreasing the probability of viral export from Asia. To further explore this hypothesis, we conducted a sensitivity analysis focused on two more recent periods that correspond approximately to the emergence in China of classical North American swIAVs (1990–2013) and avian-origin swIAVs from Europe (2000–2013), using an ‘epoch’ extension of the diffusion model²². We find that the volume of live swine is still the only well-supported predictor of viral migration for both periods (Supplementary Table 4), including when swIAVs are thought to be endemic at high levels in Asia as well as Europe and North America. In addition to the relatively low number of highly supported migration events during 2000–2013 (Fig. 2), transitions involving singleton viruses or clades that do not have high bootstrap support also contribute to the signal over this restricted time period, including migrations across the relatively porous US-Canada border and between the US/Canada and South Korea.

Predicted spatial dissemination of swIAVs

To explore how the network of global live swine trade may drive movements of swIAVs beyond the ten countries for which whole-genome sequence data was available, we used data on pairwise live swine trade between 146 countries to simulate the patterns of viral dissemination under different epidemiological scenarios. Fig. 6 explores the predicted spatiotemporal spread of a new swIAV lineage that hypothetically originates in swine in five countries with large swine populations: Canada, China, France, Mexico, and the United States. These predictions are largely consistent with the spatial movements observed in the genetic data, with a high probability of viral export from the US and Canada into Asia, and

Author Manuscript
Author Manuscript
Author Manuscript
Author Manuscript

from Europe to Asia, whereas epidemics originating from China have low probabilities of onward dissemination to other countries (Supplementary Table 5). In addition, we identified predicted connections with countries not sampled in our study, including swIAV migration from the USA and Canada to many countries in Latin America, as well as Russia, Kazakhstan, Malaysia, Thailand, and Singapore. Interestingly, our model suggests that a virus seeded in Mexican swine is comparatively less likely to disseminate to swine in other countries.

We also used our model to estimate the probability of co-invasion of European and North American swIAVs lineages, illustrating the potential for reassortment between lineages of European and North American descents, of the kind that generated the 2009 pH1N1 virus. Overall, co-invasion is strongly regionalized, with the highest probability in East and South-East Asian countries, particularly China, South Korea, and Russia (Fig. 6, Supplementary Table 5). Conversely, South Asia, the Middle East, Africa, and Australia exhibited a low probability of invasion by each of these lineages. Mid-level probabilities were found in regions with a high probability of invasion by only one of the two lineages (i.e., the North American lineage in the Americas, and the Eurasian lineage in Europe). Interestingly, these simulations reveal a low probability of co-invasion in Mexico, where pH1N1 first emerged in humans, owing to the low probability of invasion by a European swine virus in Latin America.

Discussion

The unknown origins of the swine virus that begot the 2009 H1N1 pandemic underscores the importance of understanding how influenza A viruses evolve in swine at a global scale, including regions where swIAV surveillance is lacking. Our expansive phylogenetic analysis of global swIAV sequence data demonstrates the importance of the asymmetrical nature of the global live swine trade on the global ecology and evolution of swIAVs. Using a phylogeographic GLM approach to assess the strength of specific predictors, we determine that the size of a country's swine population is not a major factor in the rate of viral export to other countries. As a notable case in point, China, which hosts the world's largest swine population, does not appear to be a major source of the viral diversity observed in other Asian countries. Rather, Japan, Thailand, Vietnam, and South Korea independently imported novel viruses from Europe and North America, most likely via long-distance live swine trade.

The reported pattern of swIAV dissemination is a reverse of a model proposed for the global spread of A/H3N2 seasonal influenza viruses in humans, in which a highly connected network of South-East Asian countries, including China, acts as a key source of viruses for Europe, North America, and other continents^{21,23}, reflecting differences in the disease and mobility patterns of humans and swine. These findings have important implications for swIAV surveillance strategies, as the relatively low levels of viral gene flow between Asian countries means that no single country in Asia can serve as a proxy for the region, including China's large swine herds. The extent of viral genetic diversity in Thailand highlights the importance of enhancing surveillance throughout South-East Asia, including countries not sampled in our study, such as Malaysia, Indonesia, Singapore, Laos, and Cambodia, as well

as undersampled countries such as Thailand, Vietnam, Japan, and South Korea. Furthermore, Russia emerged as a hotspot for invasion and co-invasion of divergent lineages in our simulations, and yet Russia has no publicly available whole-genome swIAV sequences.

The limited number of sequences from Asian countries other than China (particularly via Hong Kong, the final destination of large numbers of hogs from mainland China) reduces our ability to detect viral migration events within Asia, particularly those that do not transmit onward in swine for many years. However, the high number of viruses identified in Asia that were of North American and European origin indicates that sample bias alone cannot explain the lack of viral exchange observed between Asian countries. Analysis of larger, less-constrained data sets including all available HA swIAV sequences from Asia identified several additional viral migration events from Europe and North American swine into Asia, but only limited evidence for one additional putative connection between two Asian countries (Supplementary Figs. 10–11). However, all inferences of spatial connections must be interpreted within the context of the many countries that are unsampled and under-sampled, and long branches may conceal additional spatial movements between the origin and (final) destination location.

It is important to note that our study focused only on the international dissemination of swIAVs, and did not consider the probability of initial emergence of an epidemic within a country, which is likely to be influenced by numerous local factors related to national swine farming practices, including the size and density of farms, movements of pigs within countries, and opportunities for interspecies transmission. As demonstrated previously, the dynamics of outbreaks within a large country like the US can be complex, with different regions acting as source and sink populations for viral diversity¹⁷. Novel IAVs of human origin have emerged repeatedly in swine in countries in North America, South America, Asia, and Europe, suggesting that swine populations in these regions can sustain new epidemics²⁴. The extent of viral export from a country of origin is a product of both the national prevalence of circulating swIAVs and the volume of live swine export. In this study, we were unable to assess whether geographic differences in the prevalence of swIAVs affects large-scale viral migration, as population-level virological and serological data indicative of swIAV prevalence is available only from a limited number of study sites and time periods that are unlikely to be sufficiently representative for a global study. We therefore recognize that there are scenarios where live swine trade alone would not be a good predictor of viral migration. For example, if the major exporters of live swine (North America and Europe) did not have large endemic swIAV populations, then live swine trade alone would not be a good predictor of viral migration. This does not appear to be the case, as North America and Europe have long histories of endemic swIAV circulation and the highest volumes of outgoing international live swine trade. The apparent association between viral endemicity and trade export may not be a coincidence, as the features that enable countries in Europe and North America to export high volumes of live swine (i.e., large-scale commercial swine production) also are likely to be conducive to sustained endemic swIAV transmission. Finally, our analysis did not consider swine influenza vaccine use, which is highly heterogeneous within and between countries, and would be an important, albeit challenging, factor to integrate into future studies that consider the

interaction between the national prevalence of swIAVs, the structure of swine industries, and the global spatial dynamics of trade and viral migration.

Although it is not possible at this time to incorporate empirical data on historical differences in swIAV prevalence by region, we were able to explore the interaction of influenza virus prevalence and trade volume using our simulation model. Of particular interest was the question of whether the low levels of viral export from Asia observed in our study could be an artifact of historically lower levels of endemic swIAV activity in Asia. As a consequence, viral exports from Asian countries might be expected to rise in the future as swIAVs become endemic at higher levels throughout the region. There was no support for this hypothesis, as our simulations predicted very low rates of viral export from China to other countries even when the prevalence of swIAVs in China is set unrealistically high (e.g., 58% of Chinese swine infected when $R_0 = 1.5$). Our simulations predicted low rates of swIAV export from Japan and Thailand under similar transmissibility scenarios (Supplementary Fig. 12), with the exception of viral dissemination from Thailand to Cambodia, as these countries are trade partners. These predictions are consistent with our observation from the genetic data that swIAVs could have circulated in Japan and Thailand for many decades without substantial onward dissemination to other Asian locations sampled in our study. In addition, a sensitivity analysis of the GLM model limited to the more recent 1990–2013 and 2000–2013 periods where swIAVs were established in Asia lends further support for the importance of trade. Overall, our findings suggest that viral exchange between Asian countries with low levels of trade is unlikely to increase in the future, regardless of the potential increases in endemic swIAV activity in the region as farming practices are modernized and swine farms become larger.

Despite the importance of swine trade in the global ecology of swIAVs, it should be noted that humans may be equally, if not more, important in disseminating IAV diversity to swine herds globally²⁵. Even in the absence of international swine trade, swIAVs of human origin would likely still circulate in the majority of countries in our study, including in Asia.

Quarantine and other restrictions in international trade may have the potential to reduce the genetic diversity of swIAVs, but are not likely to prevent swIAVs from circulating in a country's swine population (Australia is a case in point²⁶). The frequency of human-to-swine transmission has been even more apparent since the 2009 H1N1 pandemic, and humans have disseminated pH1N1 viruses to swine in numerous countries that had not previously reported IAV activity in swine, including Australia^{26,27}, Brazil^{28,29}, India³⁰, Cameroon³¹, Mexico³², Nigeria³³, Sri Lanka³⁴, and several countries in Europe^{35–37}.

Unfortunately, these new data did not advance our understanding of the evolution of the pH1N1 virus during the many years of undetected circulation in swine prior to 2009. Given that the human pandemic likely emerged in Mexico³, the most parsimonious explanation is that the pH1N1 virus transmitted from swine to humans in Mexico or a nearby locality. However, extremely little swIAV sequence data is available from swine in Mexico and other parts of Latin America, and Eurasian viruses have not been detected in any part of the Americas to date. Our simulation model provides a quantitative indicator of where the reassortment event that produced the pH1N1 virus in swine was most likely to have occurred, based on the probability of invasion with both North American and European

Author Manuscript
Author Manuscript
Author Manuscript
Author Manuscript

viruses. Given limitations in our model, including the lack of information on within-country dynamics and the likelihood of initial viral emergence within seed countries, we consider the relative ranking of probabilities to be more important than their absolute values. To date, Asia is the only region where any reassortant viruses containing both North American and Eurasian virus segments have been detected³⁸, consistent with our simulations, which show a high probability of co-invasion by both North American and Eurasian swine lineages in China, South-East Asia, and Russia. However, it remains unclear how a reassortant virus that most likely emerged in swine in Asia caused its first outbreak in humans in Mexico. Given the lack of south-to-north swine trade flows in the Americas, some swIAV lineages are likely to be exclusive to Latin America^{39,40} and do not reach the United States or Canada. Strengthened surveillance in Latin America is warranted to gain a better understanding of swIAV diversity in the region.

Finally, we have focused our study on the global dynamics of influenza A viruses in swine, but our findings invite investigation of how trade, quarantine, and swine farming practices affect the spatial dynamics of other globally dispersed swine pathogens, such as PRRSV and the porcine epidemic diarrhea virus (PEDV) that emerged in US swine herds in 2013. Modeling studies rooted in pathogen sequence information, demographics, and mobility data have the power to inform global surveillance and control strategies for major animal and human disease threats.

Materials and Methods

Influenza virus sample preparation

Influenza A virus samples collected from swine via routine diagnostic submissions for the years 2002–2011 were randomly selected from the existing influenza virus archive at the University of Minnesota Veterinary Diagnostic Laboratory (UMVDL). These samples were chosen to best represent this time period and the three main geographical regions of US hog production: the Southeast region (US states of Alabama, Georgia, Kentucky, North Carolina, Tennessee, Virginia), South-central/west region (Arkansas, Colorado, New Mexico, Oklahoma, Texas), and Midwest region (Iowa, Illinois, Indiana, Kansas, Minnesota, Missouri, Nebraska). Samples from swine in Canada (2005–2011) and Mexico (2010–2011) also were selected from UMVDL, as available. Original specimen material (nasal swab supernatant or lung tissue homogenate stored at –80°C) were aliquotted from the archived samples and sent to the J. Craig Venter Institute (JCVI) in Rockville, MD for sequencing.

Influenza virus genome sequencing

The complete genomes of 240 influenza viruses collected from North American swine were sequenced at JCVI. Viral RNA was isolated using the ZR 96 Viral RNA kit (Zymo Research Corporation, Irvine, CA, USA). The influenza A genomic RNA segments were simultaneously amplified from 3 µL of purified RNA using a multi-segment RT-PCR strategy⁴¹. The M-RTPCR amplicons were sequenced using Nextera Library construction using the MiSeq platform (Illumina, Inc., San Diego, CA, USA). Additionally, M-RTPCR amplicons were sheared for 7 minutes and Ion Torrent compatible barcoded adapters were ligated to create 200 base-pair libraries that were purified and sequenced using Ion Torrent

(Life Technologies, Grand Island, NY, USA). All data sequenced for this study was submitted to the Influenza Virus Resource at the National Center for Biotechnology Information's GenBank⁴², and accession codes are available in Supplementary Table 3.

Phylogenetic analysis

In addition to the sequences generated for this study, whole-genome sequences from influenza A viruses collected in swine globally during 1960–2013 were downloaded from the Influenza Virus Resource at GenBank⁴². Viruses were removed that (a) had truncated sequences, (b) were of avian origin with no evidence of circulation in swine, (c) had unknown geographic origin, or (e) had evidence of lab errors (assessed by root-to-tip divergence using the program Path-O-Gen v1.3). Due to the disproportionately large number of swIAV sequences from the United States for the years 2009–2013, 100 of these were randomly sub-sampled.

Sequence alignments were constructed for each of the six internal gene segments (PB2, PB1, PA, NP, MP, and NS) and for the H1, H3, N1, and N2 antigenic segments separately using MUSCLE v3.8.31⁴³, with manual correction in Se-Al v2.0 (available at <http://tree.bio.ed.ac.uk/software/seal/>). Phylogenetic trees were inferred using the neighbor-joining method available in PAUP v4.0b10 for each of the ten alignments (available at <http://paup.csit.fsu.edu/>). For the PB2, PB1, and PA segments, each virus was categorized as belonging to one of the following lineages: (a) classical swine virus lineage, (b) triple reassortant ('trig') lineage, (c) avian-origin Eurasian swine lineage, (d) the pandemic H1N1 lineage that emerged in humans in 2009 and transmitted from humans to swine globally during 2009–2013 or (e) related to human seasonal influenza A viruses. For the NP, MP, and NS segments, each virus was categorized as (a) classical, (b) avian-origin Eurasian, (c) pandemic, or (d) human seasonal. No 'trig' category exists for the NP, MP, and NS segments because triple reassortant viruses contain classical virus NP, MP, and NS segments acquired through reassortment. For the H1 and N1 segments, each virus was categorized as (a) classical, (b) avian-origin Eurasian, (c) pandemic, or (d) human seasonal virus origin. All H3 and N2 segments belonged to the same category: human seasonal H3N2 virus-related.

The sequence alignment for each segment was further divided into each of these lineages. For the PB2, PB1, PA, NP, MP, NS, and N1 segments, very few (< 10) viruses were found to be of recent human seasonal virus origin, which is consistent with previous findings²⁴, so these data sets were excluded from further analyses. The pandemic H1N1 viruses that have been recently transmitted from humans to swine since 2009 remain spatially structured by country (or continent), with little evidence of long-distance migration between continents⁴⁴, and therefore sequences of pH1N1 origin were not included in further analyses. Similarly, no global migration was observed among N1 swIAV sequences that were closely related to human seasonal H1N1 viruses, and they were excluded from the study. In total, 22 segment- and lineage-specific data sets were included in the analysis (Supplementary Table 6; Supplementary Data 1). For the H3, N2, and H1 human-like (delta) lineages, human seasonal influenza virus H3, N2, and H1 sequences also were included as background. To reduce the impact of sample bias, additional phylogenies were inferred using all available full-length swIAV H1 and H3 sequence data from Asia, which included an additional 206

swIAVs from China, South Korea, Thailand, and Japan for the classical H1 segment, 191 swIAVs from China for the avian-origin Eurasian H1 segment, and 230 swIAVs from China, Thailand, Japan, Mongolia, South Korea, and Indonesia for the human seasonal virus origin H3 segment.

Phylogenetic relationships were inferred for each of the 22 data sets separately using the time-scaled Bayesian approach using MCMC available via the BEAST v1.8.0 package⁴⁵ and the high-performance computational capabilities of the Biowulf Linux cluster at the National Institutes of Health, Bethesda, MD (<http://biowulf.nih.gov>). A relaxed uncorrelated lognormal (UCLN) molecular clock was used, with a flexible Bayesian skyline plot (BSP) demographic model (10 piece-wise constant groups), and a general-time reversible (GTR) model of nucleotide substitution with gamma-distributed rate variation among sites. For viruses for which only the year of viral collection was available, the lack of tip date precision was accommodated by sampling uniformly across a one-year window from January 1st to December 31st. The MCMC chain was run separately three times for each of the data sets for at least 100 million iterations with sub-sampling every 10,000 iterations, using the BEAGLE library to improve computational performance⁴⁶. All parameters reached convergence, as assessed visually using Tracer v.1.6, with statistical uncertainty reflected in values of the 95% highest posterior density (HPD). At least 10% of the chain was removed as burn-in, and runs for the same lineage and segment were combined using LogCombiner v1.8.0 and downsampled to generate a final posterior distribution of 1,000 trees that was used in subsequent analyses.

The phylogeographic analysis considered ten locations: Argentina, Canada, China, Europe, Japan, Mexico, Thailand, United States of America, South Korea, and Vietnam. All viruses from Europe (our study included swIAV data from Belgium, Czech Republic, Denmark, France, Germany, Italy, Netherlands, Poland, Spain, and the United Kingdom) were categorized into a single spatial category due to the high level of influenza virus mixing within Europe (Supplementary Fig. 13) and the relatively low level of sampling of individual countries. Similarly, we considered Hong Kong viruses to be part of China based on genetic similarities. The location state was specified for each viral sequence, allowing the expected number of location state transitions in the ancestral history conditional on the data observed at the tree tips to be estimated using ‘Markov jump’ counts²⁰, which provided a quantitative measure of asymmetry in gene flow between regions (a representative XML file used in the analysis is provided in Supplementary Data 2). For computational efficiency the phylogeographic analysis was run using an empirical distribution of 1,000 trees²¹, allowing the MCMC chain to be run for 25 million iterations, sampling every 1,000. A Bayesian stochastic search variable selection (BSSVS) was employed to improve statistical efficiency for all data sets containing more than four location states. Maximum clade credibility (MCC) trees were summarized using TreeAnnotator v1.8.0 and the trees were visualized in FigTree v1.4.2.

Testing predictors of global swIAV migration

A generalized linear model (GLM)²¹ parameterization of the discrete phylogeographic diffusion model was employed to estimate the contribution of potential predictors to the

migration patterns of swIAVs (a representative XML file used in the analysis is provided in Supplementary Data 3; the R code used to summarize the estimates is provided in Supplementary Data 4). First, the trade value (USD) for live swine trade between countries (asymmetric) for the years 1996–2012 was obtained from the United Nations' Commodity Trade Statistics Database (available at <http://comtrade.un.org>, accessed March 20, 2014) (Supplementary Data 5). For the purposes of our study, we calculated the total trade value for each country. Data from all European countries was aggregated within the category 'Europe', and data from mainland China, Macao SAR, and Hong Kong SAR was aggregated within the category 'China'. Second, estimates of the number of live swine by country and the total number of live swine imports and exports per country were obtained for a longer time period (1969–2010) from the Food and Agriculture Organization (FAO) of the United Nations Datasets repository (available at <http://data.fao.org/datasets>, accessed March 21, 2014) (Supplementary Table 7). Again, data were aggregated across years and for Europe as well as for China. Although there is variance in trade volumes between years, some of which may also reflect variance in reporting, consistent differences in trade volume were evident among countries across years (Supplementary Fig. 14). Further, we estimated the country-specific percentage change in the pig population over the study period (ratio of the numbers of live swine in 1969 versus 2010) as an additional putative predictor of swIAVs migration. All the predictors were log-transformed and standardized prior to their specification in the GLM parameterization. We performed the GLM analysis separately for each of the six internal gene segments (PB2, PB1, PA, NP, MP, and NS) and jointly for all three swIAV lineages (avian-origin Eurasian, triple reassortant, and classical) for each segment. We achieve this, for each segment, by sharing a single GLM-diffusion model across the independent evolutionary histories of the three viral lineages. For the NP, MP, and NS segments only two lineages were included, as the triple reassortant lineage is an extension of the classical lineage for these three segments. We also excluded Argentina from the GLM analysis because no viral migration was observed between Argentina and any other country in our study. Additionally, to explore the effect of regional differences in the early establishment of swIAVs we used an 'epoch' extension of the diffusion model²² for two periods that correspond approximately to the emergence in China of classical North American swIAVs (1990–2013) and avian-origin swIAVs from Europe (2000–2013) (representative XML file available provided in Supplementary Data 6).

Meta-population model simulating the global spread of swine influenza

Next, we built a meta-population model to explore the global spread of swIAVs and identify potential geographical hotspots for reassortment between viruses originating from different regions, which may generate novel viruses with pandemic potential. We built a meta-population model to explore the global spread of swIAVs and identify potential geographical hotspots for reassortment. We employed a stochastic patch-based SIR model adapted from an earlier model for the global diffusion of human influenza⁴⁷. Each patch represents the swine population of an individual country, and patches are linked based on live swine trade movements. To calibrate the model, we obtained swine population sizes and pairwise between-country trade information for 146 countries reporting to FAO during 1969–2010 (<http://data.fao.org/datasets>; Supplementary Table 7, Supplementary Data 5), which coincides with the study period considered for phylogenetic analysis of swIAVs. We

used the averages of swine population sizes and pairwise trade volumes throughout the study period for model simulations.

The influenza simulation model is as follows. Let \mathbf{S} , \mathbf{I} , and \mathbf{R} denote vectors representing the number of susceptible, infected, and recovered swine at any time point in each of the 146 countries studied. We let $\mu = 1/5$ denote the daily probability that an individual recovers (so that the infectious period is 5 days^{48,49}), and $\beta\mathbf{I}$ the daily per-capita rate of infection from infectious individuals within the same country. Here, β varies between countries; it is a vector scaled such that the effective reproduction number $R_{\text{eff}} = \beta\mathbf{N} / \mu$ is the same in all countries, where \mathbf{N} is the vector of swine population sizes. We use an R_0 of 1.5 in main analyses, consistent with limited information on swine influenza dynamics^{48,49}. The per-capita rate of contacts with infectious swine from other countries is given by $\mathbf{G}^*\mathbf{I}$, where \mathbf{G} represents the 146*146 matrix of between-country coupling.

To build \mathbf{G} , we first create \mathbf{T} , a 146*146 matrix with off-diagonal elements based on empirical live swine trade and zeros along the diagonal. We then rescale \mathbf{T} by the estimated trade coefficients of the phylogeographic GLM model, as the GLM model suggests the relationship between trade and viral migration is not linear (but results are qualitatively similar with no rescaling). Following past work⁴⁷, the rescaled matrix \mathbf{T}' is then tuned by a free parameter, c , which governs the amount of international vs. domestic contacts between swine, while at the same time allowing conversion of empirical swine trade data (provided in \$ amount by FAO) into actual population movements. Tuning parameter c allows obtaining realistic time course of infection, with global epidemics lasting between several months to several years, in line with (limited data available on) the global spread of past swine outbreaks. Our final coupling matrix is $\mathbf{G} = c\mathbf{G}'$, where c is such that the maximum element of the coupling matrix is lower than 10^{-3} .

We use a spatially-extended chain-binomial system to update the progression of the epidemic in each patch⁴⁷:

$$\begin{aligned} S_{t+1} &= S_t - W_t \\ I_{t+1} &= I_t + W_t - V_t \\ R_{t+1} &= R_t + V_t \\ W_t &= \text{binomial}(S_t, 1 - e^{-\beta * (I_t + G * I)}) \\ V_t &= \text{binomial}(I_t, \mu). \end{aligned}$$

Here, \mathbf{W}_t is the daily incidence of swine influenza (ie the number of new cases), and \mathbf{V}_t is the number of new ‘recovereds’.

In simulations, the epidemic is initialized by infecting 5 swine in a predetermined seed country; we explored various scenarios with seeds in countries of the Americas, Europe and Asia. After the first infection occurs in each country, we draw a multinomial to determine the source of the infection, from a normalized vector $\mathbf{G}^*\mathbf{I}$. For each scenario, involving a given source country (e.g., US, Canada, UK, France, China), we ran 1,000 simulations, allowed to run over a three year time period, and assess the probability of swine flu invasion in each non-source country, and its most likely source of infection. We conducted sensitivity

analyses with higher and lower values of the free parameter c and R_0 , which mostly affected the time course of the global epidemic and the synchronicity of epidemics across locations, but did not change dramatically the identification of hotspots countries for onward spread. To explore the probability of reassortment between viruses originating from North America and Europe, we ran 1000 independent simulations of epidemics starting in North America (USA and Canada), and in each the 10 European countries with largest swine populations, and compute the co-invasion probability in country i , following:

$$P.coinv.i = [1 - \prod_{j \text{ source countries in North America}} (1 - p.inv_{i,j})] * [1 - \prod_{k \text{ source countries in Europe}} (1 - p.inv_{i,j})],$$

where $p.inv_{i,k}$ is the probability that country i is invaded when the outbreak is seeded in country k .

Estimates were then used to produce risk maps for swIAV invasion and co-invasion using software available in the R package (<http://www.r-project.org/>).

Supplementary Material

Refer to Web version on PubMed Central for supplementary material.

Acknowledgments

The authors wish to thank Drs. Sagar Goyal and Devi Patnayak, along with Wendy Wiese, Becca Wheeldon, and Lotus Smasal at UMVDL for their virology work, and Rebecca Halpin, Nadia Fedorova, Xudong Lin, and Timothy B. Stockwell at the J. Craig Venter Institute for their assistance in viral sequencing. This manuscript was prepared while DEW was employed at the J. Craig Venter Institute. Partial support for this work was provided by a grant from the Saskatchewan Ministry of Agriculture contract number C70077. This work was supported in part by the Multinational Influenza Seasonal Mortality Study (MISMS), an on-going international collaborative effort to understand influenza epidemiology and evolution, led by the Fogarty International Center, National Institutes of Health, with funding from Office of Pandemics and Emerging Threats at the U.S. Department of Health and Human Services [AR, MIN, CV]. This project has also been funded in part with federal funds from the National Institute of Allergy and Infectious Diseases, National Institutes of Health, Department of Health and Human Services under the [contract number HHSN272200900007C]. PL, MAS, and AR acknowledge funding from the European Union Seventh Framework Programme [FP7/2007-2013] under Grant Agreement no. 278433-PREDEMICS and ERC Grant agreement no. 260864. ECH is supported by an NHMRC Australia Fellowship (AF30).

References

1. Garten RJ, et al. Antigenic and genetic characteristics of swine-origin 2009 A(H1N1) influenza viruses circulating in humans. *Science*. 2009; 325:197–201. [PubMed: 19465683]
2. Smith GJD, et al. Origins and evolutionary genomics of the 2009 swine-origin H1N1 influenza A epidemic. *Nature*. 2009; 459:1122–1125. [PubMed: 19516283]
3. Lemey P, Suchard M, Rambaut A. Reconstructing the initial global spread of a human influenza pandemic: A Bayesian spatial-temporal model for the global spread of H1N1pdm. *PLoS Curr*. 2009; 1:RRN1031. [PubMed: 20029613]
4. Koen JS. A practical method for field diagnosis of swine diseases. *Am J Vet Med*. 1919; 14:468–470.
5. Zhou NN, et al. Genetic reassortment of avian, swine, and human influenza A viruses in American pigs. *J Virol*. 1999; 73:8851–8856. [PubMed: 10482643]
6. Karasin A, Carman S, Olsen C. Identification of human H1N2 and human-swine reassortant H1N2 and H1N1 influenza A viruses among pigs in Ontario, Canada (2003 to 2005). *J Clin Microbiol*. 2006; 44:1123–1126. [PubMed: 16517910]

7. Vincent AL, et al. Characterization of a newly emerged genetic cluster of H1N1 and H1N2 swine influenza virus in the United States. *Virus Genes*. 2009; 39:176–85. [PubMed: 19597980]
8. Ottis K, Sidoli L, Bachmann P, Webster RG, Kaplan MM. Human influenza A viruses in pigs: isolation of a H3N2 strain antigenically related to A/England/42/72 and evidence for continuous circulation of human viruses in the pig population. *Arch Virol*. 1982; 73:103–108. [PubMed: 6184032]
9. Vijaykrishna D, et al. Long-term evolution and transmission dynamics of swine influenza A virus. *Nature*. 2011; 473:519–522. [PubMed: 21614079]
10. Takemae N, et al. Antigenic variation of H1N1, H1N2 and H3N2 swine influenza viruses in Japan and Vietnam. *Arch Virol*. 2013; 158:859–876. [PubMed: 23435952]
11. Poonsuk S, Sangthong P, Petcharat N, Lekcharoensuk P. Genesis and genetic constellations of swine influenza viruses in Thailand. *Vet Microbiol*. 2013; 167:314–26. [PubMed: 24095146]
12. Song D, et al. A novel reassortant canine H3N1 influenza virus between pandemic H1N1 and canine H3N2 influenza viruses in Korea. *J Gen Virol*. 2012; 93:551–554. [PubMed: 22131311]
13. Nelson MI, et al. Genomic reassortment of influenza A virus in North American swine, 1998–2011. *J Gen Virol*. 2012; 93:2584–2589. [PubMed: 22993190]
14. Zell R, et al. Novel reassortant of swine influenza H1N2 virus in Germany. *J Gen Virol*. 2008; 89:271–276. [PubMed: 18089751]
15. Nelson MI, Vincent AL, Kitikoon P, Holmes EC, Gramer MR. Evolution of novel reassortant A/H3N2 influenza viruses in North American swine and humans, 2009–2011. *J Virol*. 2012; 86:8872–8878. [PubMed: 22696653]
16. Duceatz MF, et al. Multiple reassortment between pandemic (H1N1) 2009 and endemic influenza viruses in pigs, United States. *Emerg Infect Dis*. 2011; 17:1624–9. [PubMed: 21892996]
17. Nelson MI, et al. Spatial dynamics of human-origin H1 influenza A virus in North American swine. *PLoS Pathog*. 2011; 7:e1002077.
18. Shi M, et al. The spread of type 2 Porcine Reproductive and Respiratory Syndrome Virus (PRRSV) in North America: a phylogeographic approach. *Virology*. 2013; 447:146–54. [PubMed: 24210109]
19. Anderson TK, et al. Population dynamics of cocirculating swine influenza A viruses in the United States from 2009 to 2012. *Influenza Other Respi Viruses*. 2013; 7(Suppl 4):42–51.
20. Minin VN, Suchard MA. Counting labeled transitions in continuous-time Markov models of evolution. *J Math Biol*. 2008; 56:391–412. [PubMed: 17874105]
21. Lemey P, et al. Unifying Viral Genetics and Human Transportation Data to Predict the Global Transmission Dynamics of Human Influenza H3N2. *PLoS Pathog*. 2014; 10:e1003932. [PubMed: 24586153]
22. Bielejec F, Lemey P, Baele G, Rambaut A, Suchard MA. Inferring heterogeneous evolutionary processes through time: from sequence substitution to phylogeography. *Syst Biol*. 2014; 63:493–504. [PubMed: 24627184]
23. Russell CA, et al. The global circulation of seasonal influenza A (H3N2) viruses. *Science*. 2008; 320:340–6. [PubMed: 18420927]
24. Nelson MI, et al. Introductions and evolution of human-origin seasonal influenza A viruses in multinational swine populations. *J Virol*. 2014; 88:10110–9. [PubMed: 24965467]
25. Nelson MI, Vincent AL. Reverse zoonosis of influenza to swine: new perspectives on the human-animal interface. *Trends Microbiol*. 2015; 10.1016/j.tim.2014.12.002
26. Holyoake PK, et al. The first identified case of pandemic H1N1 influenza in pigs in Australia. *Aust Vet J*. 2011; 89:427–431. [PubMed: 22008120]
27. Deng Y, Iannello P, Smith I. Transmission of influenza A (H1N1) 2009 pandemic viruses in Australian swine. *Influ Other Respi Viruses*. 2012; 6:42–47.
28. Biondo N, et al. Genomic analysis of influenza A virus from captive wild boars in Brazil reveals a human-like H1N2 influenza virus. *Vet Microbiol*. 2014; 168:34–40. [PubMed: 24238665]
29. Schaefer R, Zanella JRC, Brentano L, Vincent AL, Ritterbusch GA, Silveira S, Caron L, M N. Isolation characterization of a pandemic H1N1 influenza virus in pigs in Brazil. *Pesqui Vet Bras*. 2011; 31:761–767.

30. Nagarajan K, et al. Influenza A H1N1 virus in Indian pigs & its genetic relatedness with pandemic human influenza A 2009 H1N1. *Indian J Med Res.* 2010; 132:160–167. [PubMed: 20716816]
31. Njabo KY, et al. Pandemic A/H1N1/2009 influenza virus in swine, Cameroon, 2010. *Vet Microbiol.* 2012; 156:189–192. [PubMed: 21963416]
32. Escalera-Zamudio M, et al. Characterization of an influenza A virus in Mexican swine that is related to the A/H1N1/2009 pandemic clade. *Virology.* 2012; 433:176–182. [PubMed: 22921315]
33. Meseke CA, Odaibo GN, Olaleye DO. Detection and isolation of 2009 pandemic influenza A/H1N1 virus in commercial piggery, Lagos Nigeria. *Vet Microbiol.* 2014; 168:197–201. [PubMed: 24321146]
34. Perera HKK, et al. Swine influenza in Sri Lanka. *Emerg Infect Dis.* 2013; 19:481–484. [PubMed: 23621918]
35. Hofshagen M, Gjerset B, Er C. Pandemic Influenza A(H1N1)v: Human to pig transmission in Norway. *Euro Surveill.* 2009; 14:1–3.
36. Nokireki T, Laine T, London L, Ikonen N, Huovilainen A. The first detection of influenza in the Finnish pig population: a retrospective study. *Acta Vet Scand.* 2013; 55:69. [PubMed: 24047612]
37. Bánya K, et al. Genome sequence of a monoreassortant H1N1 swine influenza virus isolated from a pig in Hungary. *J Virol.* 2012; 86:13133. [PubMed: 23118459]
38. Lam TTY, et al. Reassortment events among swine influenza A viruses in China: implications for the origin of the 2009 influenza pandemic. *J Virol.* 2011; 85:10279–10285. [PubMed: 21795347]
39. Cappuccio, Ja, et al. Outbreak of swine influenza in Argentina reveals a non-contemporary human H3N2 virus highly transmissible among pigs. *J Gen Virol.* 2011; 92:2871–2878. [PubMed: 21849519]
40. Schaefer R, et al. A human-like H1N2 influenza virus detected during an outbreak of acute respiratory disease in swine in Brazil. *Arch Virol.* 2014; 159(10):2223–2223-z
41. Zhou B, et al. Single-reaction genomic amplification accelerates sequencing and vaccine production for classical and Swine origin human influenza a viruses. *J Virol.* 2009; 83:10309–13. [PubMed: 19605485]
42. Bao Y, et al. The influenza virus resource at the National Center for Biotechnology Information. *J Virol.* 2008; 82:596–601. [PubMed: 17942553]
43. Edgar RC. MUSCLE: multiple sequence alignment with high accuracy and high throughput. *Nucleic Acids Res.* 2004; 32:1792–7. [PubMed: 15034147]
44. Nelson MI, Gramer MR, Vincent AL, Holmes EC. Global transmission of influenza viruses from humans to swine. *J Gen Virol.* 2012; 93:2195–2203. [PubMed: 22791604]
45. Drummond AJ, Suchard MA, Xie D, Rambaut A. Bayesian phylogenetics with BEAUti and the BEAST 1.7. *Mol Biol Evol.* 2012; 29:1969–73. [PubMed: 22367748]
46. Suchard MA, Rambaut A. Many-core algorithms for statistical phylogenetics. *Bioinformatics.* 2009; 25:1370–6. [PubMed: 19369496]
47. Viboud C, et al. Synchrony, waves, and spatial hierarchies in the spread of influenza. *Science.* 2006; 312:447–51. [PubMed: 16574822]
48. Romagosa A, et al. Vaccination of influenza a virus decreases transmission rates in pigs. *Vet Res.* 2011; 42:120. [PubMed: 22185601]
49. Wong KK, et al. Transmissibility of variant influenza from Swine to humans: a modeling approach. *Clin Infect Dis.* 2013; 57(Suppl 1):S16–22. [PubMed: 23794727]
50. Robinson TP, et al. Mapping the global distribution of livestock. *PLoS One.* 2014; 9:e96084. [PubMed: 24875496]

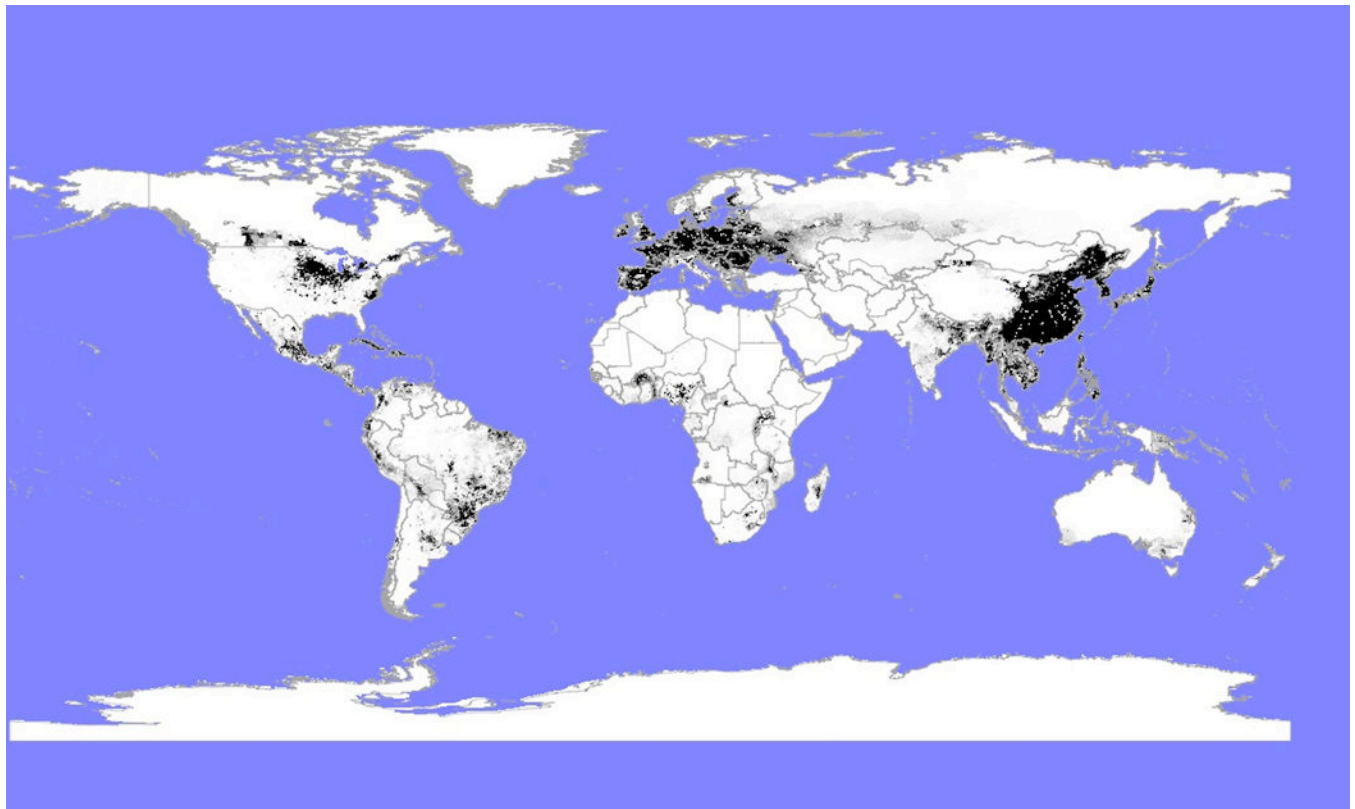


Fig. 1. Modeled global swine distributions

Digital layers from Gridded Livestock of the World (GLW) (version 2.01)⁵⁰, downloaded from the publically available Livestock Geo-Wiki database (<http://www.livestock.geo-wiki.org>) and manually edited in QGIS v.1.7.0. Swine densities are represented by black shading.

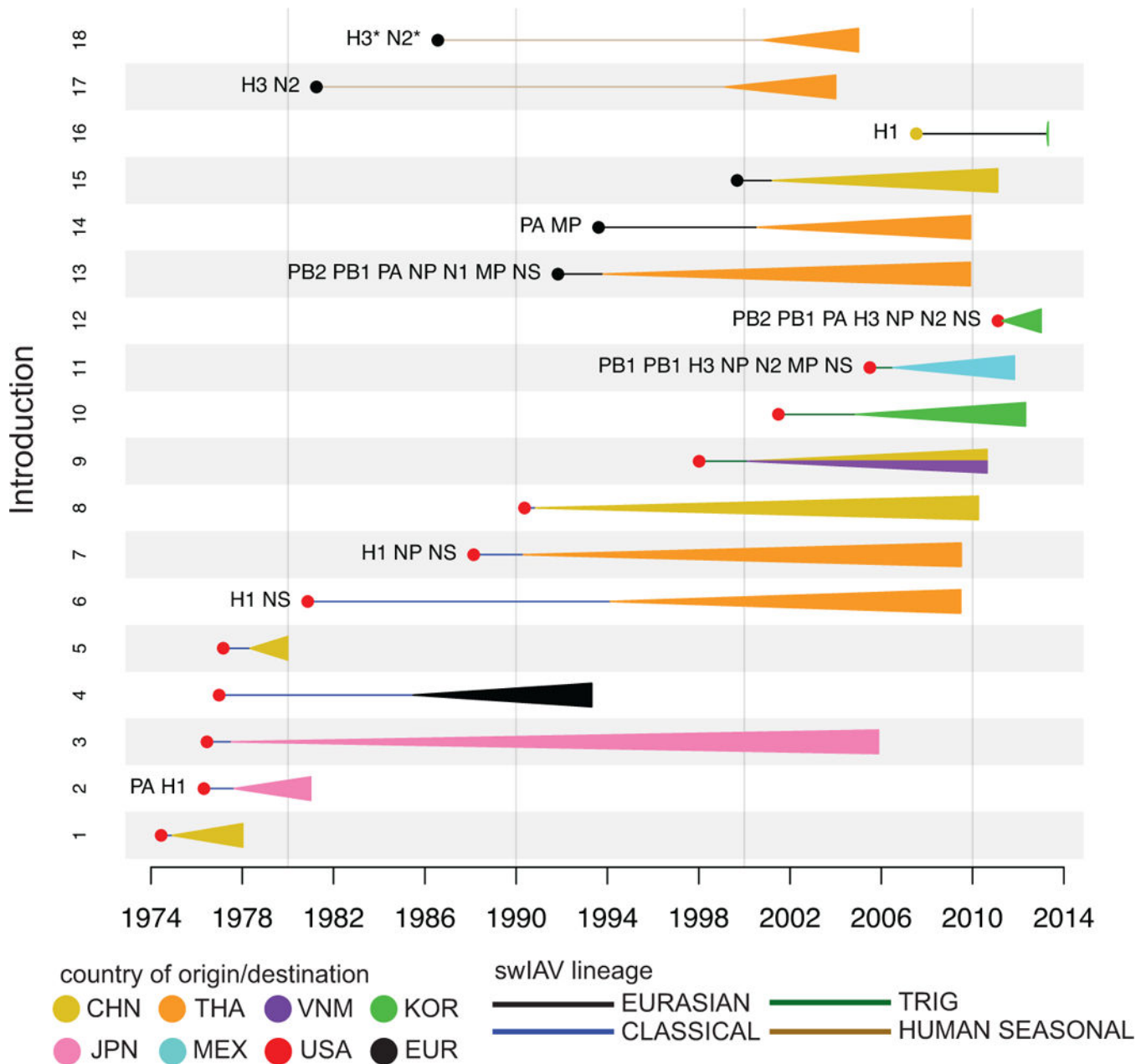
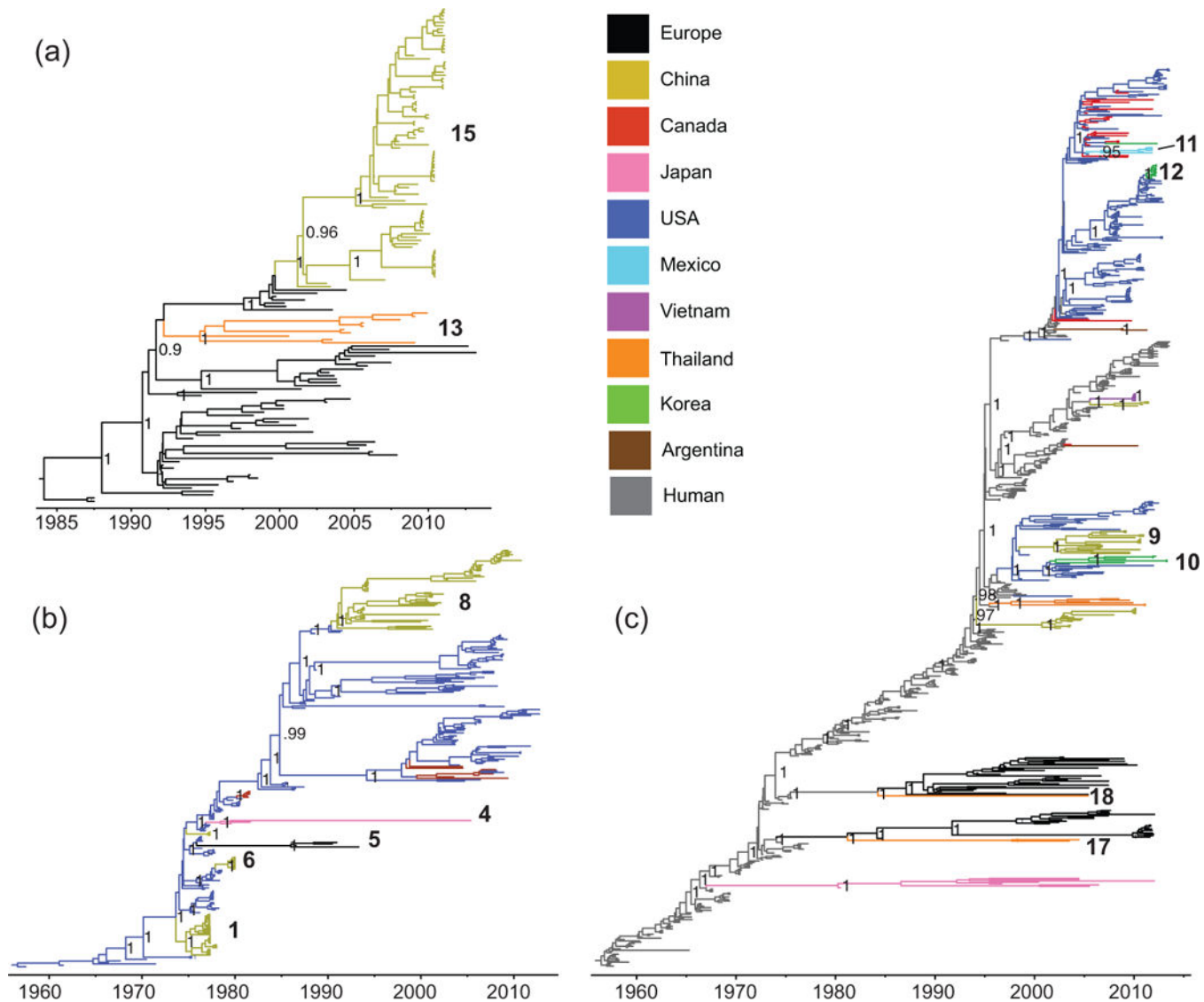


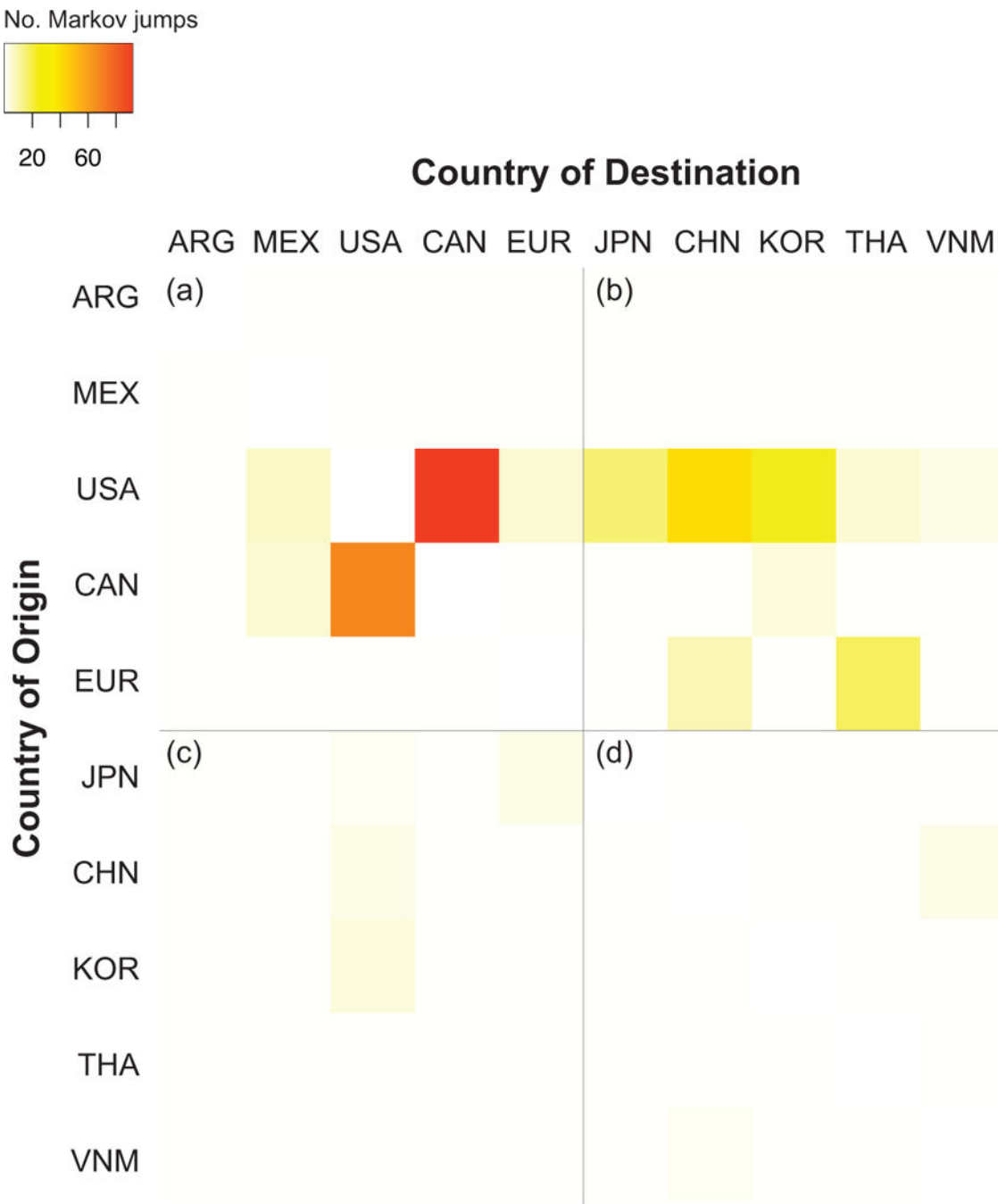
Fig. 2. Inter-continental migration events of swIAVs

Circles represent the country of origin, based on the estimates summarized in the MCC tree, and are shaded accordingly. Lines represent the inferred time period of inter-continental transmission, within a level of uncertainty, inferred from the estimated date of ancestral nodes on the MCC tree. Triangles represent clades resulting from onwards transmission of the introduced viruses, are shaded by the country of destination, and extend as far forward in time as the most recently sampled virus. Numbers of introduction (1–18) correspond to the clade numbers on the phylogenies (Fig. 3 and Supplementary Figs. 1–7). The asterisks indicate that additional HA and NA swIAV sequence data was used to estimate the timing of introduction 18. Countries/regions are abbreviated as follows: CHN = China (including

Hong Kong SAR and Taiwan), THA = Thailand, VNM = Vietnam, KOR = South Korea, JPN = Japan, MEX = Mexico, and EUR = Europe.

**Fig. 3. MCC trees of the NA lineages in swine**

Time-scaled Bayesian MCC trees inferred for the NA segment for the three major swine virus lineages: (a) avian-origin Eurasian N1 swIAV lineage, the (b) classical N1 swIAV lineage, and the (c) multiple human seasonal virus-origin N2 swIAV lineages circulating in swine. Branches of human seasonal H3N2 influenza virus origin are shaded grey in (c), while branches associated with viruses from swine are shaded by country of origin: Argentina = brown; Canada = red; China (including Hong Kong SAR and Taiwan) = yellow; Europe = black; Japan = pink; Mexico = light blue; South Korea = green; Thailand = orange; USA = dark blue; Vietnam = purple. Posterior probabilities > 0.8 are included for key nodes, and international migration events that are supported by high posterior probabilities and long branch lengths are labeled according to Fig. 2.

**Fig. 4. Heat-map of swIAV migration between locations**

Countries are listed in order of increasing geographical distance from Argentina (ARG). MEX = Mexico, USA = United States, CAN = Canada, EUR = Europe, JPN = Japan, CHN = China (including Hong Kong SAR and Taiwan), KOR = South Korea, THA = Thailand, VNM = Vietnam. The intensity of the color (red = high; white = low) reflects the number of ‘Markov jump’ counts inferred over the totality of phylogenies (all segments, all lineages) from one location to another (asymmetrical). Markov jump counts measure the number of inferred location state transitions, modelled by a continuous-time Markov chain process, that

occur along the branches of the phylogeny. For clarity the heat-map has been divided into four sections representing (a) viral migration events within the Americas and between the Americas and Europe; (b) migrations from the Americas/Europe to Asia; (c) migrations from Asia to the Americas/Europe; and (d) migrations between Asian countries.

Author Manuscript

Author Manuscript

Author Manuscript

Author Manuscript

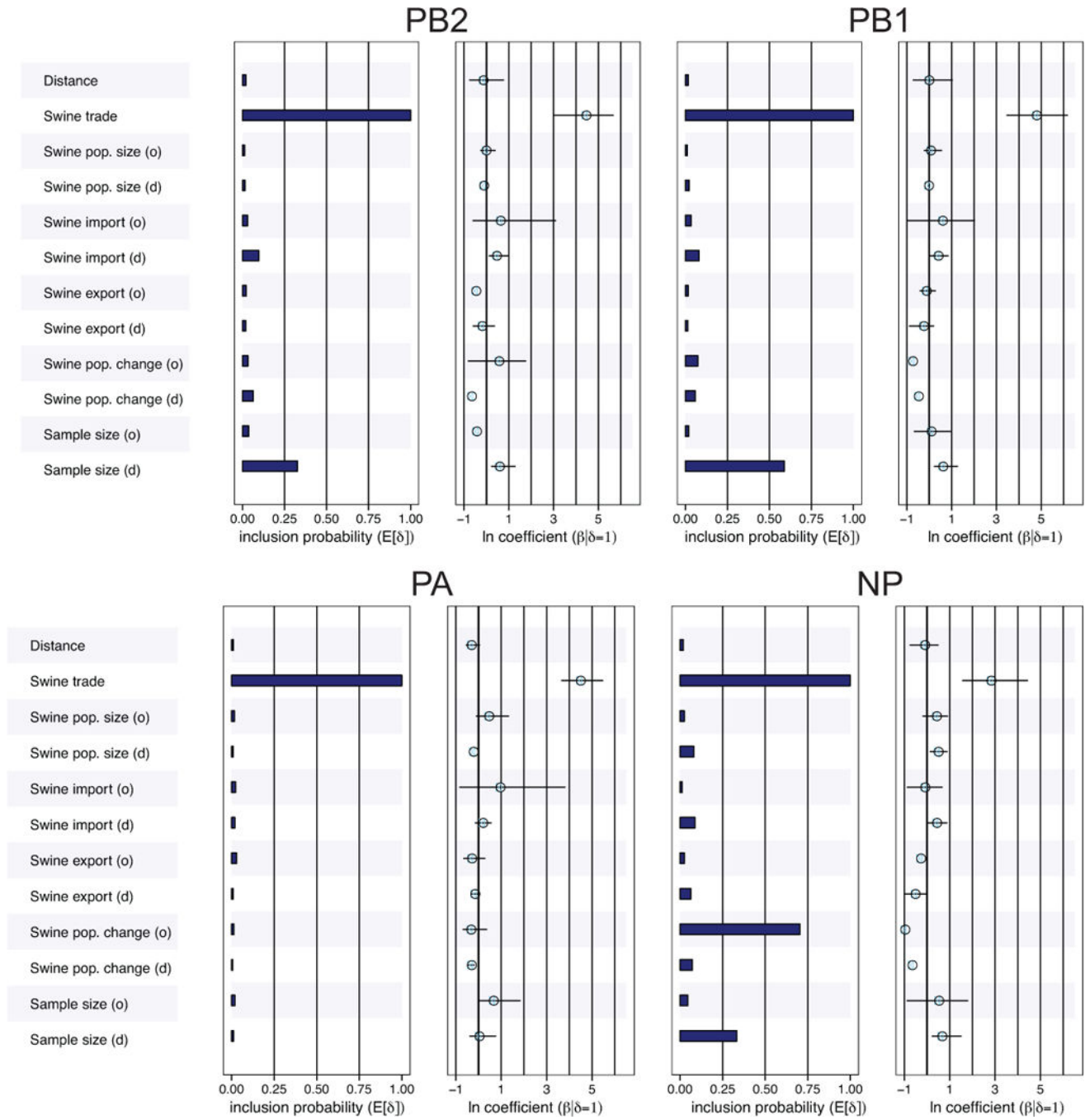


Fig. 5. The support and contribution of swIAV diffusion predictors among 9 countries

Twelve predictors were considered: geographical distance (km), volume of live swine trade, 1996–2012 (USD), swine population size for the years 1969–2010, the total number of imports of live swine during 1969–2010, the total number of swine exports during 1969–2010, the percent change in swine population size from 1969–2010, and the number of sequences available from a given country for our analysis. ‘O’ refers to the swine population of origin, and ‘d’ refers to the swine population of destination. Support for each predictor is represented by an inclusion probability that is estimated as the posterior expectation for the

indicator variable associated with each predictor ($\mathbf{E}[\delta]$). The contribution of each predictor is represented by the mean and credible intervals of the GLM coefficients (β) on a log scale conditional on the predictor being included in the model ($\beta|\delta=1$). See Supplementary Fig. 8 for MP and NS results.

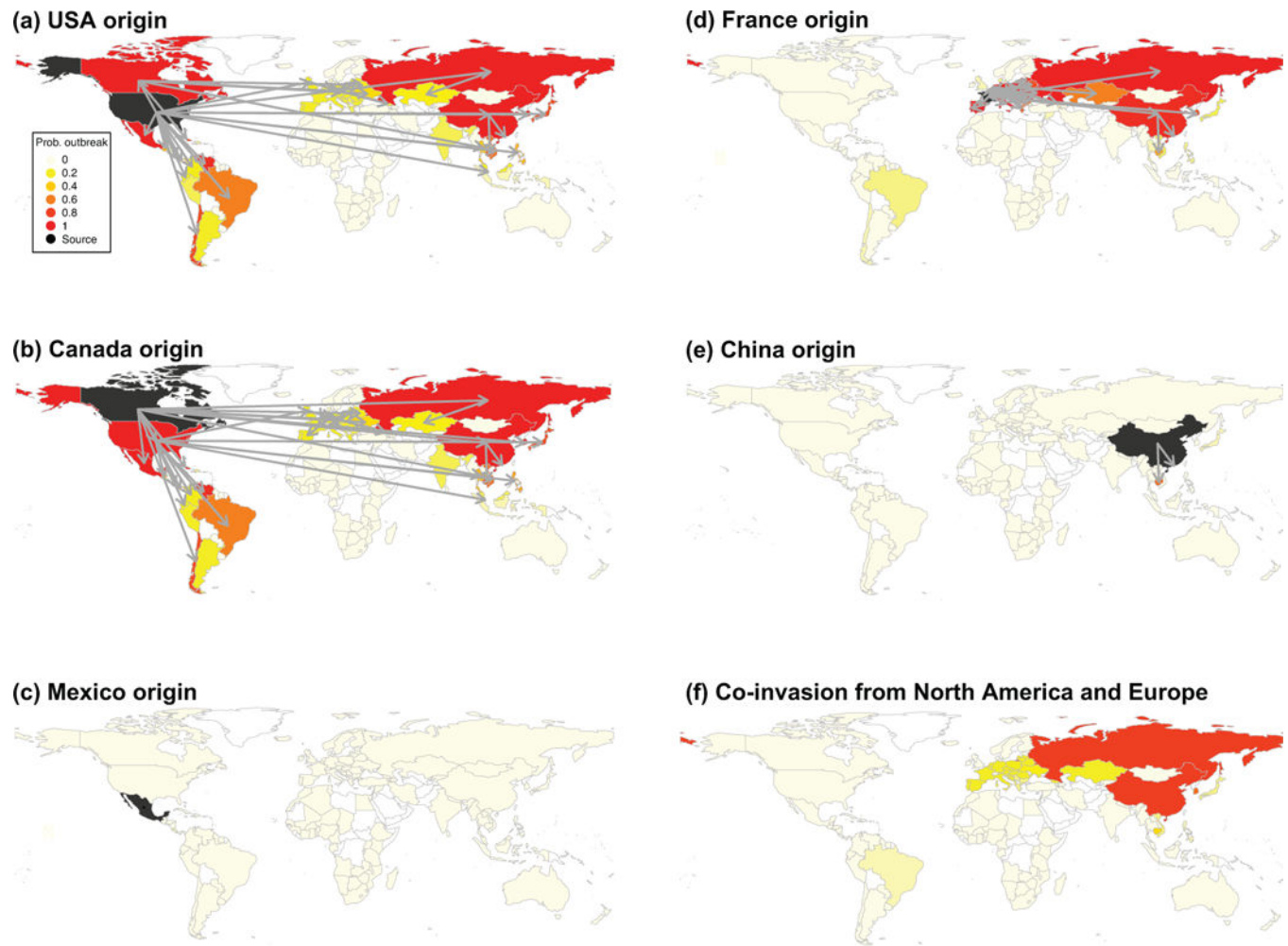


Fig. 6. Maps of simulated spread of influenza viruses via live swine trade flows

Simulated spread of an influenza virus from 5 seed countries (shaded in black) to 146 countries for which live swine trade is available from the United Nations Commodity Trade Statistics Database (available at <http://comtrade.un.org>) (a–e). Probability of an outbreak in the invaded country is shaded from white (probability of 0) to red (probability of 1). The probability of co-invasion by both a virus seeded in North America (Canada and the United States) and Europe also is shaded from white (probability of 0) to red (probability of 1) (f). Arrows represent the direction of viral dissemination for countries with a probability of an outbreak > 0.25 (see Supplementary Table 5 for a complete list of all outbreak probabilities by country).